Laser and Particle Beams (2007), *25*, 557–566. Printed in the USA.

DOI: 10.1017/S0263034607000675

Lasing properties and nonlinearities of dyes under high power pumping

M. MILANI,[1] L. FERRARO,[1] F. CAUSA,[2] AND D. BATANI[3]

[1]Department of Material Sciences, Milano-Bicocca University, Milan, Italy
[2]Department of Electronic and Electrical Engineering, University of Bath, UK
[3]Department of Physics, Milano-Bicocca University, Milan, Italy

(RECEIVED 4 February 2007; ACCEPTED 23 July 2007)

Abstract

Nitrogen lasers have been used for many years to make dye solutions lase. A nitrogen laser, which transverse electrical discharge in gas at atmospheric pressure has been built in our laboratory. It has been characterized and applied to pump different dyes: Rhodamine 6G, Coumarin 440, DOTCI, and pyranine in simple "on axis" geometric configuration. It has been shown that pyranine can lase in the absence of any optical external mirror cavity, this happens at very low threshold, and in different solvents. Dyes under consideration can be grouped into two major classes according to their lasing behavior independently on their concentration in the solvent: Rhodamine 6G and DOTCI can lase both axially or transversally and Coumarin 440 and pyranine can lase only axially. Other intriguing features have been observed that span from simultaneous multiple beam generation, to super fluorescence and to distribute axial pumping of dye solutions. A preliminary basis for understanding and controlling such processes is the spatial energy distribution and the energy density of the beam.

Keywords: Dyes; Lasing properties; Laser radiation Nitrogen laser

INTRODUCTION

Nitrogen lasers have been used for many years as optical pumps for dye lasers (Fitzsimmons *et al.*, 1976; Schwab & Hollinger, 1976; Godard, 1974; Jeunehomme & Duncan, 1964; Bennett & Dalby, 1959). A transverse electrical discharge in gas at atmospheric pressure (TEA) nitrogen laser ($\lambda = 337.1$ nm) was built (Milani *et al.*, 1999, 2000). The laser system and emitted pulses have been thoroughly characterized, and used to pump quartz cells of various sizes filled with a number of dye solutions.

Nitrogen laser radiation consists of isolated pulses of coherent radiation. The laser action begins when a molecule of nitrogen, at room temperature, absorbs energy by colliding with an electron in the discharge. The gas quickly becomes strongly absorbing. In fact, the laser turns itself off even though there are still excited molecules left; nitrogen lasers are self-terminating, the turnoff time being rather fast, and usually less than 10 ns.

Address correspondence and reprint requests to: D. Batani, [1]Department of Physics, Milano-Bicocca University, Milan, Italy. E-mail: batani@mib.infn.it

The laser action in nitrogen can be activated by a mechanism, which almost instantaneously, sends a huge current of electrons, at a high voltage laterally, through a column of gas (whose pressure is critical for pulse duration). A proper and effective switching mechanism, which can handle tens of thousands of amperes within nanoseconds, turns out to be quite simple both in principle and in construction.

Research and application of nanosecond pulsed laser beams find novel interest in transient processes analysis, for instance, in plasma dynamics, and in micromachining, where nanosecond pulses give better performances than femtosecond pulses, since there is sufficient time for the pulse energy to be distributed to the target substrate in the form of heat (Bashir *et al.*, 2007; Wolowski *et al.*, 2007; Chouffani *et al.*, 2006; Miley *et al.*, 2005).

THE NITROGEN LASER

The nitrogen laser was built in our laboratory according to a novel layout. It is characterized by an open cavity and works at atmospheric pressure (TEA laser). Pumping is obtained by a low-impedance flat-plate Blumlein pulse generator (Fig. 1).

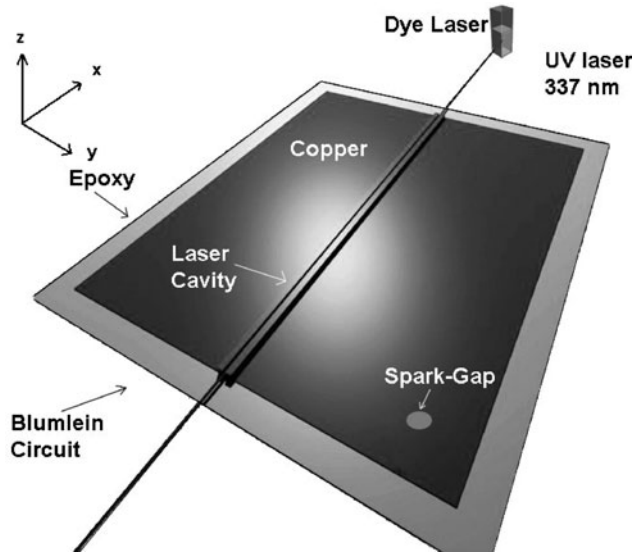

Fig. 1. Overall laser layout.

The presence of a traveling wave cavity allows high pumping levels and stimulated emission efficiency, still with significant stability of the pulse spatial profile. Typical dimensions of the laser setup is 130×110 cm^2, cavity length is 100 cm, and cavity cross-section is 1×0.5 cm^2 on average; the cavity cross-section is tapered and of variable geometry to ensure single facet emission, and to control pulse repetition rates, threshold, and pulse energy. Performances of the output pulse can be summarized as follows: repetition rate up to 80 Hz, pulse length on the order of 0.5 ns, 1–5 mJ pulse energy, 2 MW peak power, and 0.5 J/cm^2.

An energy measurement (OPHIR Nova laser power/energy monitor; head PE25), at the minimal value of energy for electric breakdown (the minimal distance between the electrodes of spark gap is 20 mm); on 400 pulses at 3 Hz repetition rate is reported in Table 1. Actual values can be compared (Figs. 2a, 2b, 2c) with data in the literature that are well summarized in Strohwald and Salzmann (1976) and Bergmann (1979). Applications of this laser to life sciences were investigated (Milani *et al.*, 1999, 2000). The laser pumping system is a mirrorless cavity filled by free (grade 5) flowing nitrogen at atmospheric pressure. The electric discharge is triggered transversally to the channel axis uniformly by a Blumlein circuit. The resulting pumping process is the single-pass traveling wave type that is the most effective for the given cavity length in the absence of mirrors.

Table 1. *Single pulse energy for nearly parallel electrodes at a distance of 4 mm yielding a very low value of backward/forward ratio*

	Beam energy (μJ)
Minimum	88
Maximum	300
Average	170
St. Dev.	50.5

BEAM PROFILE CHARACTERIZATION

A method is chosen for characterizing the spatial profile of the nitrogen laser beam that makes use of commercially available color photographic films (Fujicolor 100). To

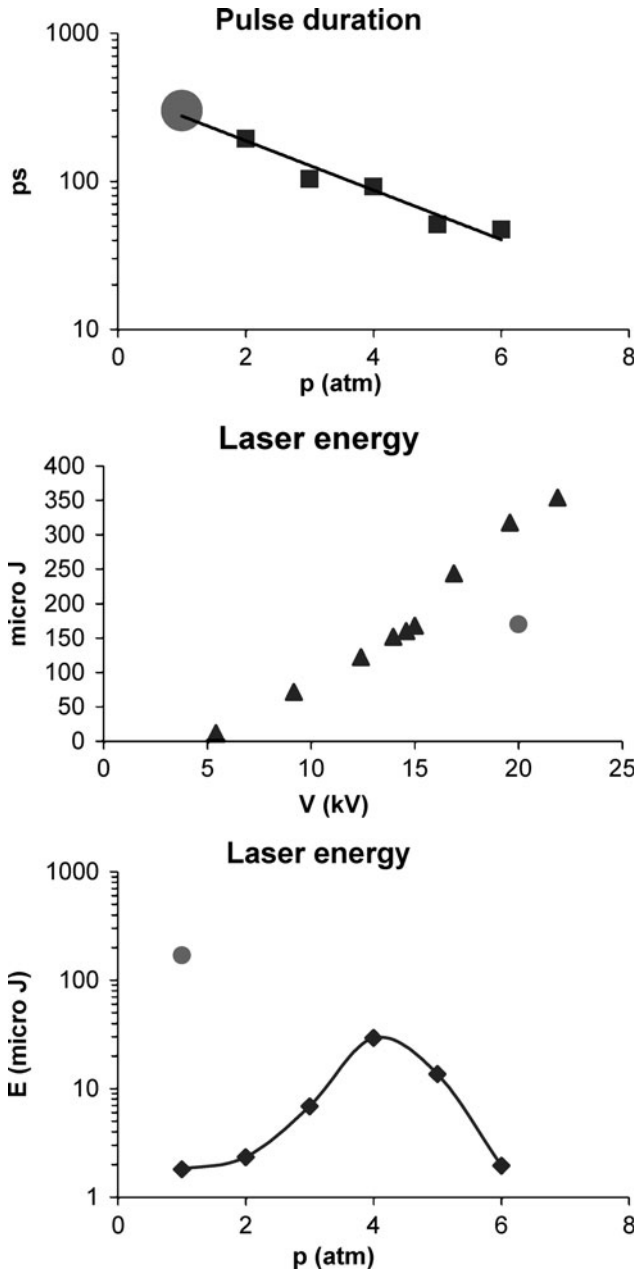

Fig. 2. Comparison between literature data and value measured in the laboratory. ● Our value. ▲ ■ ◆ Values of Strohwald and Salzmann (1976) and Bergmann (1976).

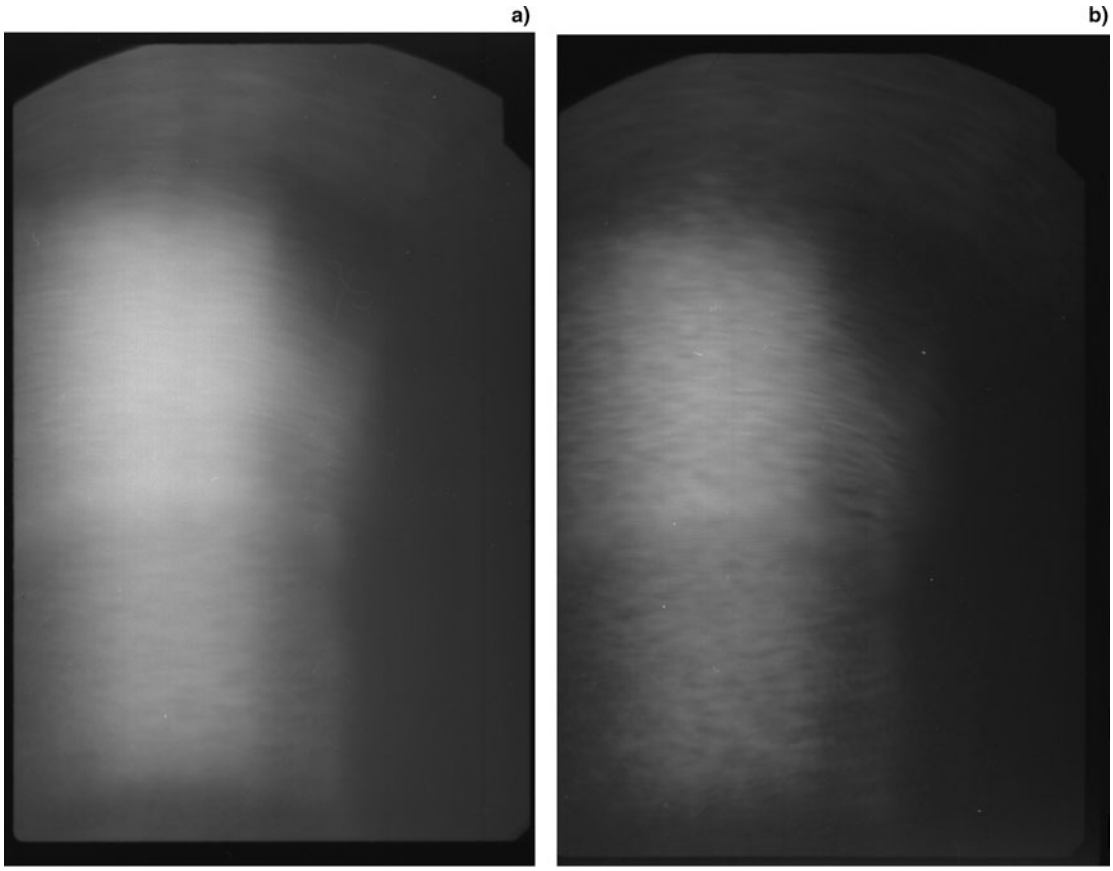

Fig. 3. (**a**) A picture a records the sequence of four pulses. (**b**) A picture of a single non polarized pulse.

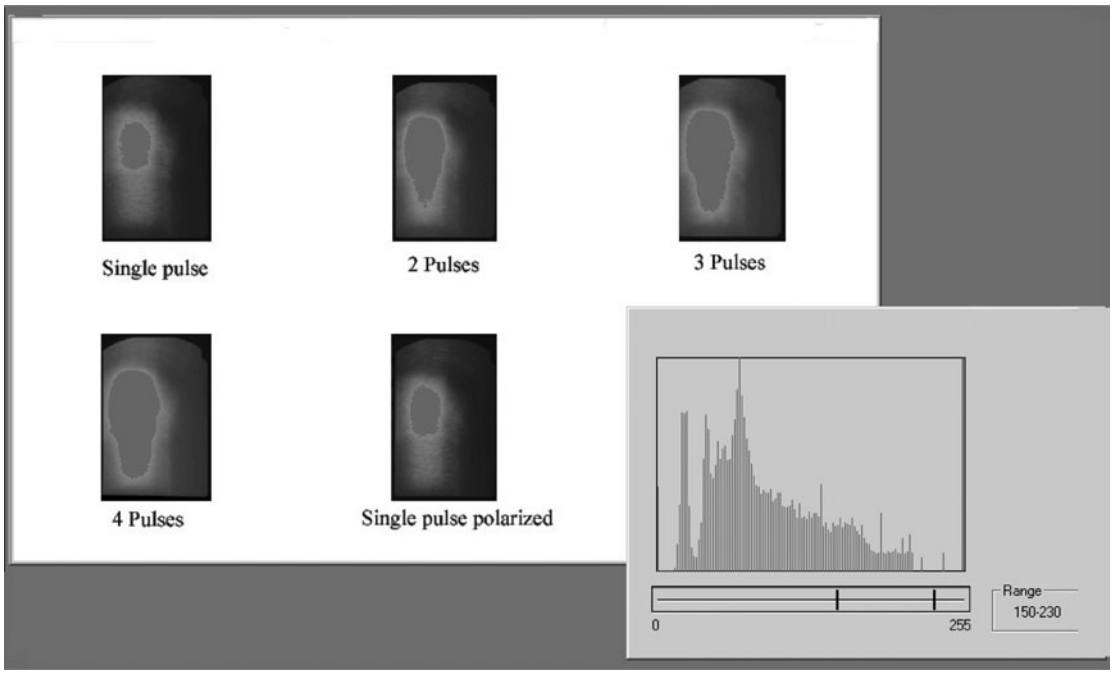

Fig. 4. One screenshot of Image Tool analysis. Five images were processed in a threshold range 150–230 and the program makes the report of data in selected areas.

determine whether the procedure is viable for this type of analysis, we evaluated the response of the film to the laser beam, since the commercial film is certified only for visible light, together with its saturation limits, linear regime response and threshold for a given wavelength. This method was required to evaluate energy distribution in the cross-section of the laser beam. However, the chosen two-dimensional section is quite large when searching for the evaluation of wavefront changes in a laser pulse; therefore, the energy distribution is averaged on the whole wavefront.

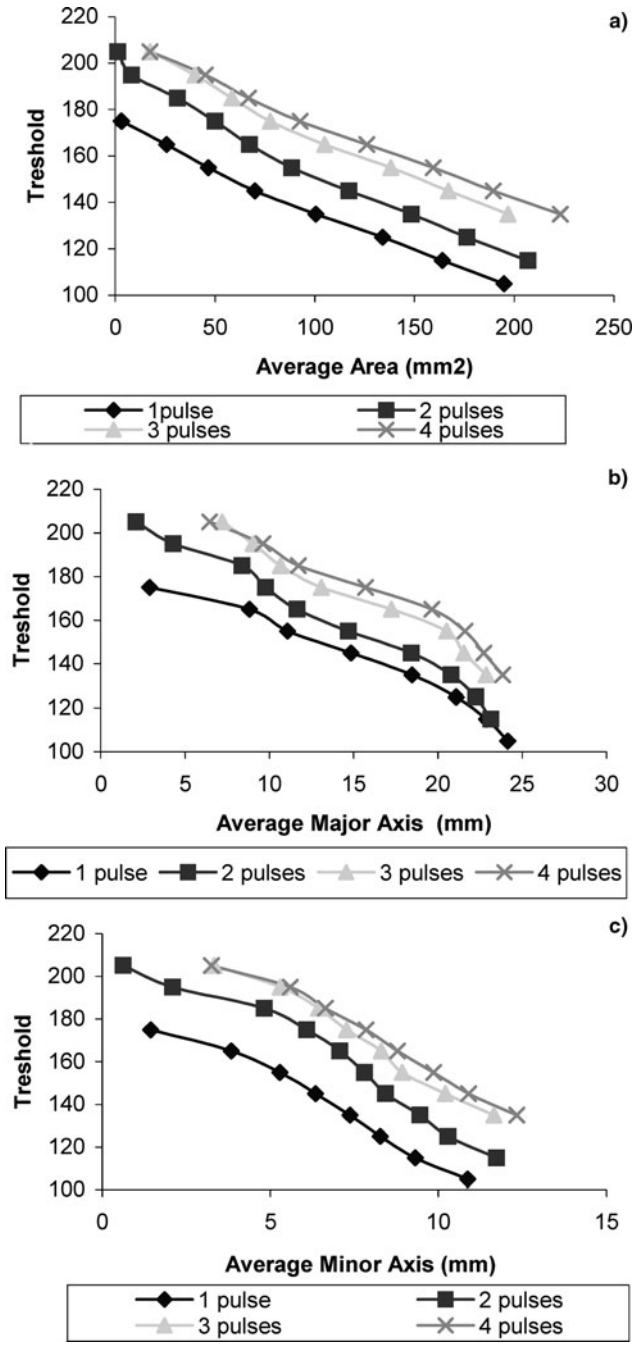

Fig. 5. Average values of minor axis (**c**), major axis (**b**) and area (**a**) of the laser spot for images recording different numbers of laser pulses.

Actually, optical elements like lenses or mirrors between laser, and detector typically modify the beam profile, and gives rise to absorption. Therefore, the acquisition of the images was performed by a camera without lenses, operating in the dark. Images were acquired in groups of three, to characterize the film response to 1 pulse, 2 pulses, 3 pulses, and 4 pulses sequence, at 1 Hz repetition rate (Figs. 3a, 3b). Subsequently, the response to single pulse suitably polarized by a polarizer has been recorded. In data analysis, we consider the average on the values of the three images in every sequence. The obtained images were straightforwardly scanned directly from the negative films (Epson Perfection 1200S, 1200 dpi) after standard developing procedure. We observed that the print out of the negative has fan out effects on the information stored in the negatives.

Two commercial softwares for the elaboration of the images were used: Paint Shop 8.0 and Image Tool for Windows 3.0. Scanning has been performed at 24 bits and in a successive step, before image elaboration, the dynamic range has been reduced to 8 bits, so to have black and white images (physically more strictly linked to the monochromatic nature of the beam) with 255 grey levels. In both cases, we subdivide the monochromatic images in 255 levels of a grayscale, with the assumption that at an increase of the grey level corresponds to an increase of the intensity of energy absorbed by the film in a selected spot. It is important to recall that commercial films are not certified for monochromatic UVA pulses of such energy, power, and

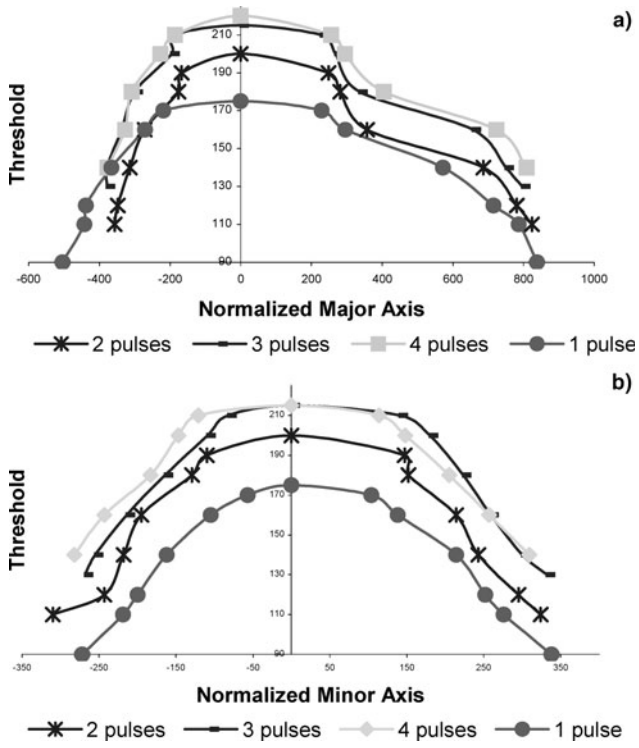

Fig. 6. The bell shape of the beam seen along minor (**a**) and major (**b**) axis.

time duration. With the tool "Threshold," we locate the image zone where the grey level is highest, and than a threshold value is selected. Height and width of the selected zone are evaluated. Iterations of the process for different threshold values give the beam profile.

Paint shop allowed a survey of the data by aiming the pointer onto the border of beam profile and reading the coordinates of such points. With Image Tool, we refined the technique of acquisition and carried out data analysis with the tool's "Analyze," with the advantage of simultaneously processing more images (see Fig. 4) that were previously converted to grayscale. An advantage of Image Tool is the possibility to obtain information on the actual dimensions of the image in a direct way by the tool's "calibrate spatial measurements;" so that one can exploit the information that a 35 mm film (actual dimensions 24 mm × 36 mm) was used. In Figure 5, the diagrams obtained by the elaboration of the images are reported.

Mechanical stability of the system, reproducibility of data, and spatial energy distribution can be established by data made available via the above described sequence of operations on films. It is interesting to observe the beam profile reconstruction through the data via Paint Shop as presented in Figure 6, which leads to a stable well defined beam section profile.

After finding the coordinates of maximum intensity and take it for reference as the zero of the plot, the data related to this point were normalized. A bell shaped behavior appears showing a greater density of energy at the center of the beam. Therefore, when the laser beam is used as a pump for a dye laser, it will pump an ellipsoidal zone in the plane transversal to the propagation direction. The stability of the overall laser setup can be assessed by the strong similarities of profiles for $n > 1$ pulses and single pulse profile. Finally, the diagrams obtained with Image Tool are compared for differently polarized pulses (Fig. 7), and the conclusion can be drawn that the laser pulse has no significant polarization.

The selected method used with the photographic film for the determination of the profile of the beam with subsequent file developing and digitalization, proved to be effective, and

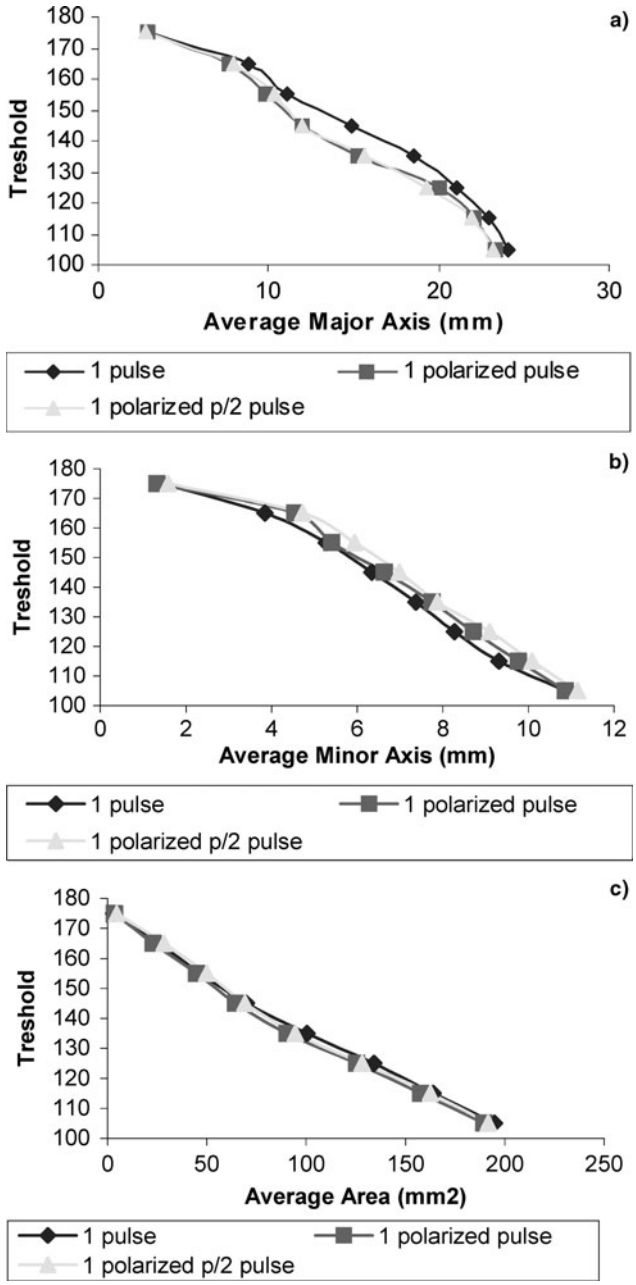

Fig. 7. Average of major axis length (**a**) minor axis length (**b**) and area (**c**) of the spot of whole pulse, and of the polarized pulses at 0° and $\pi/2$; for sake of comparison they have been all normalized to the same maximum value.

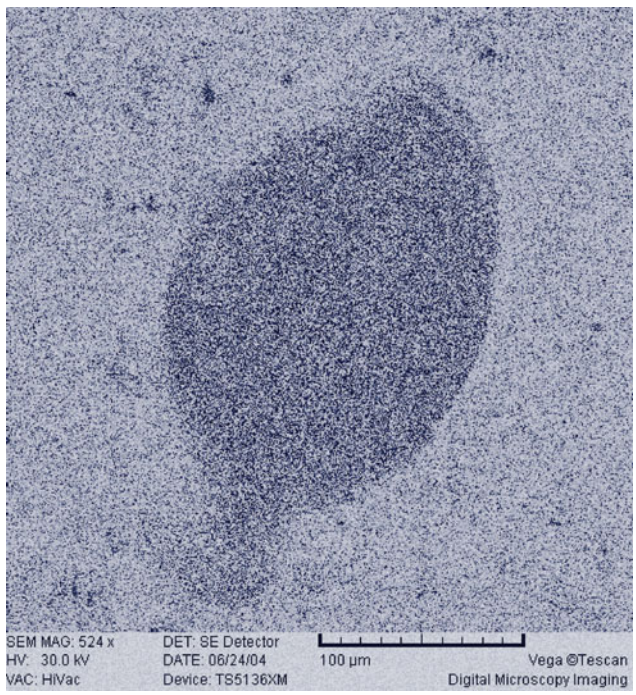

Fig. 8. (Color online) The effect of the beam directed onto the surface of the mylar sheet covered with iron oxide.

rich in information. The film has a good dynamic range of the intensity of the beam: no saturation is observed in single pulse recording, while still some dynamic range for the procedure is left. Moreover, the diagrams do not point to any significant difference as far as the polarization of the beam is concerned; that is, as expected the beam is not polarized.

Another complementary technique was used to further characterize the beam profile. The beam was focused by a spherical lens on a target Mylar sheet covered by iron oxide and keeping the target slightly out of focus to avoid damage to the target. The surface of the target was subsequently imaged using a scanning electron microscope (SEM) (Fig. 8). Under the same operation conditions but with the target in the focal point, the target surface was seriously damaged. The cross-section of the beam seen on the target surface shows that the major axis has the dimension on the order of 100 μm, which confirms that the beam has an elliptic profile, with a slight asymmetry as it was visible in the film, and in the derived plots obtained by digital operations in the scanned image.

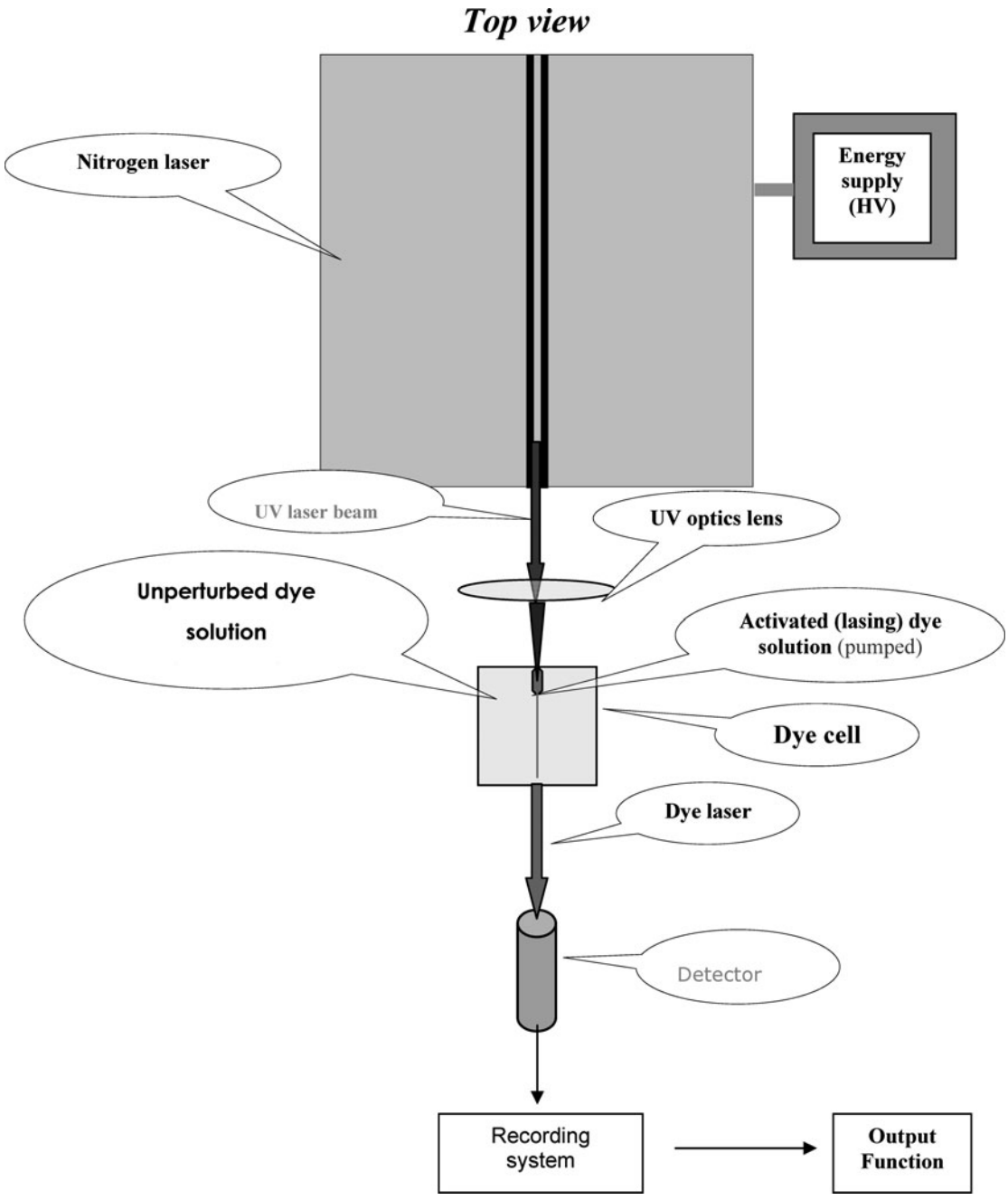

Fig. 9. The UV nitrogen beam enters the dye (Rhodamine 6G) solution cell, making it to lase in the visible range at the usual wavelength. Top view along the xy plane, see also Figure 1.

DYE LASER OPERATIONS

Nitrogen laser beam can be used to pump a cell containing a selected concentration of a dye solution, obtaining an emission wavelength dependent on the dye molecule (Duarte & Hillman, 1985). The in-house developed nitrogen laser was used to pump four different dyes: Pyranine, Rodamine 6G, Coumarin 440, and DOTCI (3,3'-Dimethyloxatricarbocyanine iodide). The experimental layout is presented in Figure 1 and Figure 9. The dye solution is contained in a quartz cuvette of 4 ml volume, square cross-section, and inner path of 10 mm. Solvents used are methanol for Rhodamine 6G, Coumarin 440, and DOTCI, while water was used for Pyranine. In the case of the pyranine molecule, the laser beam develops transversally to the pumping axis (the pumping beam being focused on the cell by means of a cylindrical lens). No lasing action can take place along the pumping axis. Rodamine 6G, Coumarin 440, and DOTCI present interesting novel geometrical features in beam formation (Figs. 10a, 10b, and 11) that are related to the type of focusing lens, and lasing activity can be observed that is coaxial with the pumping UV beam (Brivio *et al.*, 1994, 1993; Bogdanov & Zaitsev, 2001; Lin & Zhang, 1987; Bos, 1981). Furthermore, threshold concentrations can be evaluated for the prepared solutions.

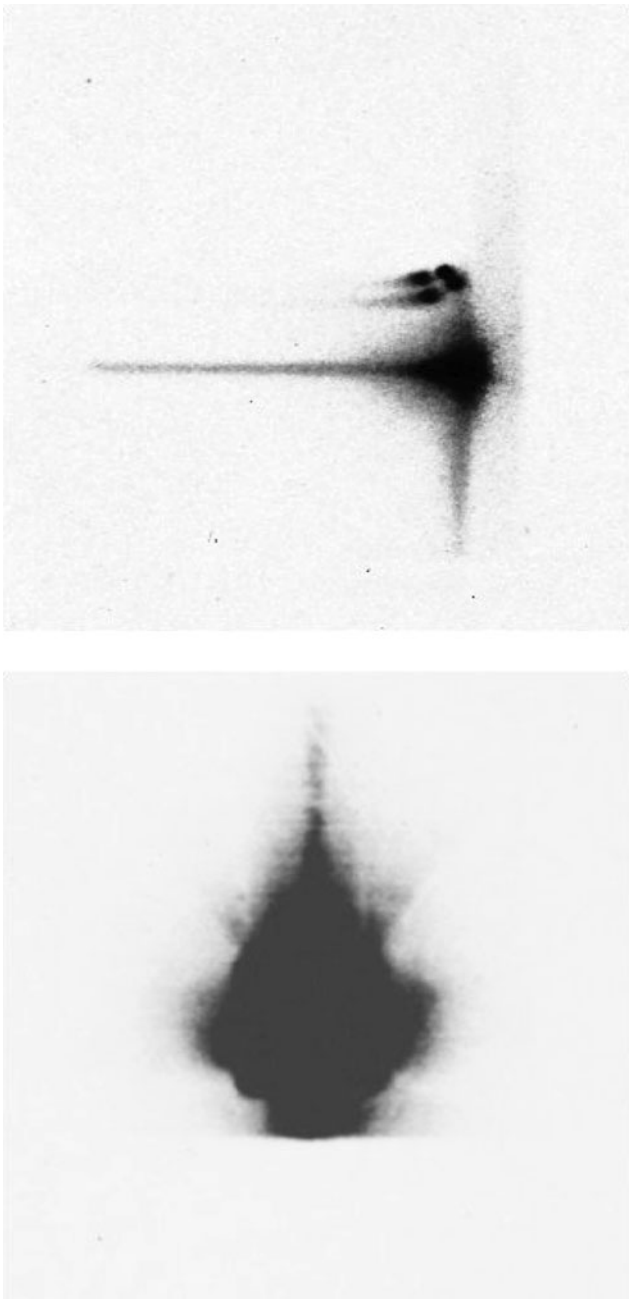

Fig. 10. Red (Fig. 9a) and green regions of rhodamine emission spectrum (top view) [we have found digitally these regions using software filter].

RESULTS

Using a spherical lens, the UV laser beam was focused on the first facet of the cuvette, obtaining a pumping length of 1 mm along the y direction. Different behaviors have been observed depending on the type of dye used (Rhodamine 6G, DOTCI, Pyranine, and Coumarin 440). In the case of Rhodamine 6G and DOTCI, pumping gives transverse or longitudinal laser beams, by translating by tens of microns, the position of the cuvette with respect to the focal point of the UV beam along the pumping direction. For a selected focal position, a simultaneous longitudinal and transversal emission is recorded. The analysis of the polarization properties by a polarizer shows that transverse beams acquire polarization, while the longitudinal one remains unpolarized. For Coumarin 440 and Pyranine, emission is observed only

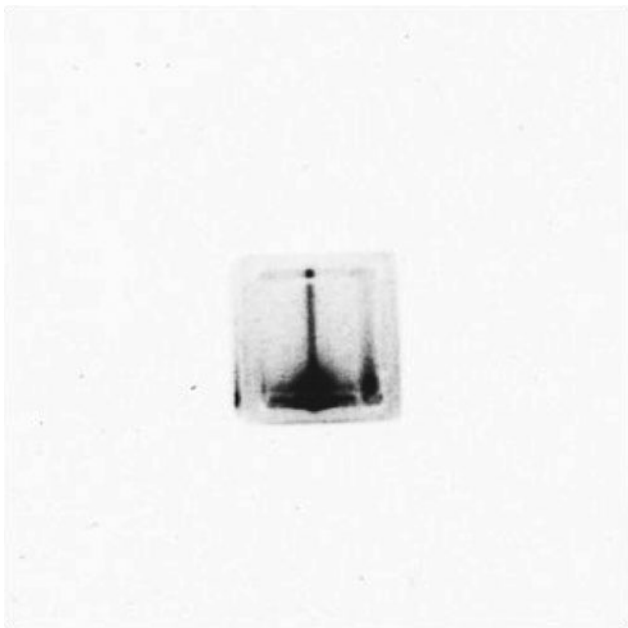

Fig. 11. Scheme of the orientation of polarized and unpolarized beams with respect to the pump beam from the nitrogen laser depending on the relative position of the focal spot with respect to the front facet of the cuvette.

along the pumping axis. These results are summarized for sake of clarity in Figures 12a and 12b. We can observe: (1) the presence of multi wavelength beam light emission, highlighted by the yellow and red images (Figs. 10a, 11). (2) The presence of light in a region outside the cuvette, where only red component is retained (Fig. 10a). (3) The simultaneous presence of many laser beams in the cuvette where only the green component is retained (Fig. 11). (4) The coexistence of axial and transverse lasing action.

In the literature, transverse lasing action of Coumarin is reported, but this takes place in complex optical systems where mirrors and gratings are presents, while in the reported setup, the only cavity is the one generated by cuvette walls. Moreover, here is reported and characterized for the first time, the lasing action of the molecule pyranine (8-hydroxy-1,3,6-pyrenetrisulfonate trisodium salt) in water solution when pumped by a nitrogen laser (Figs. 13a, 13b, 13c). Some authors (Rifani *et al.*, 1995; Kahr & Gurney, 2001) mention lasing action of pyranine: "Laser action may be of pyranine in alluminosilicate glasses" (Kahr & Gurney, 2001). "Laser action of K_2SO_4

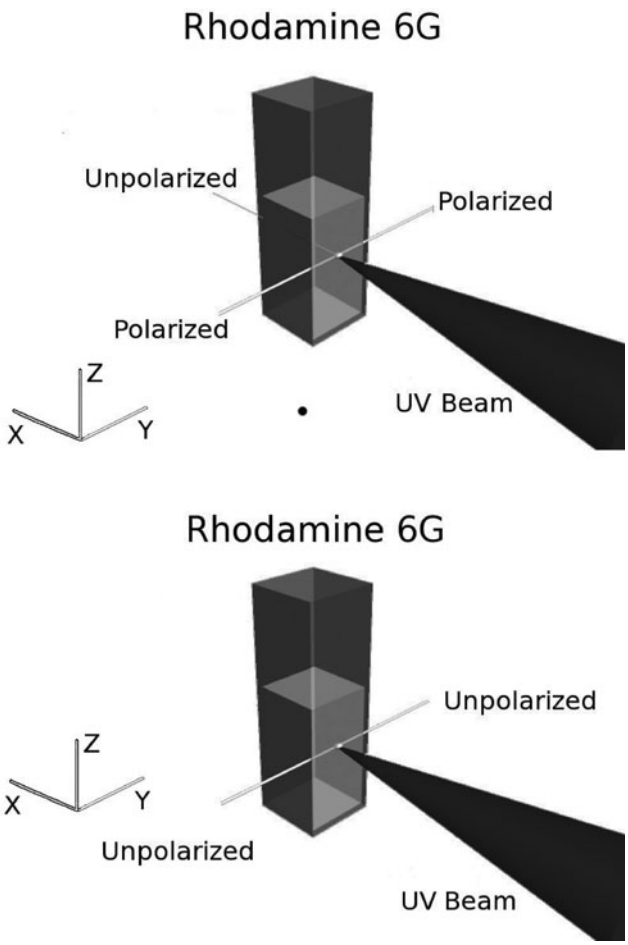

Fig. 12. Scheme of the orientation of polarized and unpolarized beams with respect to the pump beam from the nitrogen laser, depending on the relative position of the focal spot with respect to the front facet of the cuvette.

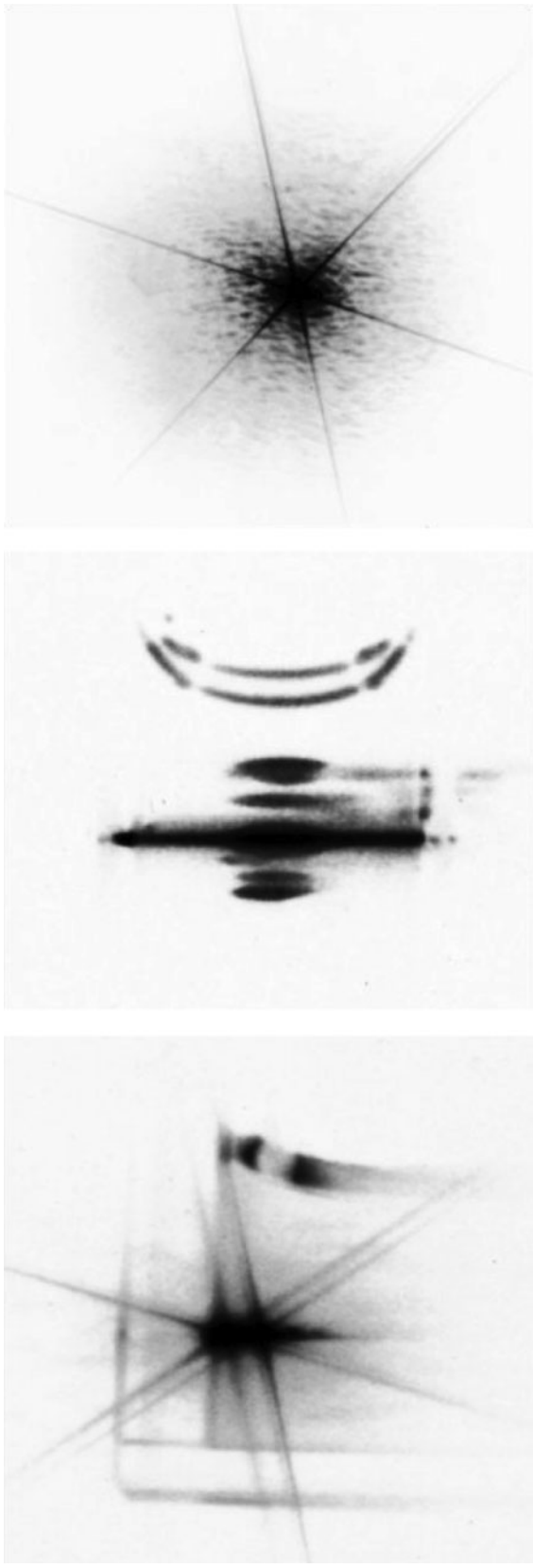

Fig. 13. The pictures represents: (**a**) the front end of the dye laser beam generated by a pyranine solution when pumped by the nitrogen laser (plane y-z, according to Fig. 1). (**b**, **c**) two side views (plane x-y and x-y, respectively, according to Fig. 1).

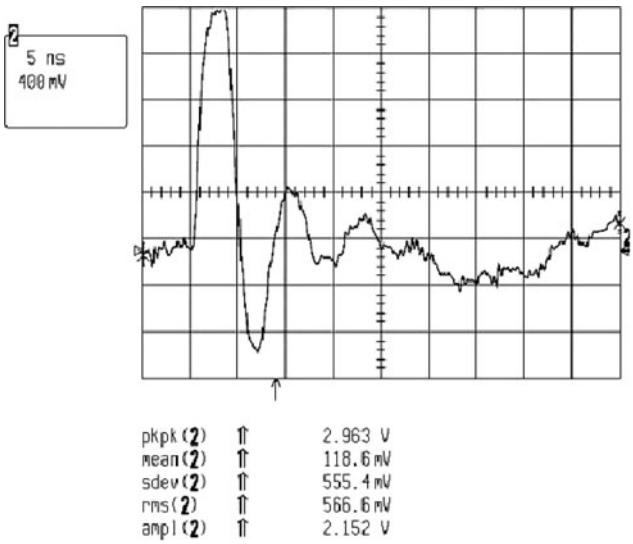

Fig. 14. Pulse length has been measured with a photodetector APX65 connected to le Croy 9384CM, 1 GHz oscilloscope with le Croy PPO94, 4 G samples/s adaptor. The pulse duration is shorter than 500 ps.

crystals doped with pyrene and Rhodamine dyes" but no reports are given for the lasing characteristics; threshold and pumping of such dye (Kahr & Gurney 2001). The threshold for pyranine laser action is very low as can be derived from a comparison with Rhodamine 6G performances under similar exposure to laser light pulses. The pH of the pyranine solution plays a fundamental role; it induces changes in fluorescence wavelength, although no changes appear in the laser emission frequency. A limiting factor to the investigation is that turbidity develops as a consequence of the transition from the basic form to the acid one. Even in this case, no external optical cavity created by external mirrors has been used, and the cuvette has been tilted by some degrees with respect to z-axis to avoid back reflections inside the cavity.

CONCLUSIONS

First, the nitrogen laser beam has been investigated and its main properties characterized. The laser pulse is shorter than 0.5 ns (see Figure 14) and has an average energy of 0.170 mJ. By means of a photographic technique, we have found that the beam has a stable, bell-shaped profile; this implies that when the beam is used for dye laser pumping, the pumped region has most likely an elliptical cross-section. The photographic technique is reliable for single pulse recording, and the absence of beam polarization can be safely assessed.

Lasing action was demonstrated for pyranine in basic water solution transversally to the pumping axis. For the Rhodamine 6G, we found two behaviors associated to a diffuse fluorescence in the red region of the spectrum: the appearance of simultaneous collimated beams of high brilliancy in the red region with transversal and axial directions with respect to the pumping axis; this most likely is laser action or at least the proof of cooperative optical processes driven by the combination of dye concentration and power density of the pumping beam. Future activity will be devoted to the identification of the nature of cooperative dye-photon processes at work together with the investigation of the role of shape and size of the dye solution pumped region.

REFERENCES

Bashir, S., Rafique, M.S. & Ul-Haq, F. (2007). Laser ablation of ion irradiated CR-39. *Laser Part. Beams* **25**, 181–191.

Bennett, R.G. & Dalby, F.W. (1959). Experimental determination of the oscillator strength of the first negative bands of N^{2+}. *J. Chem. Phys*. **31**, 434–441.

Bergmann, E.E. (1979). UV TEA Laser with 760-torr N2. *Appl. Phys. Lett*. **28**, 84–85.

Bogdanov, A.A. & Zaitsev, A.I. (2001). Generation of transmitted and reflected waves in induced super radiance. *Laser Phys.***11**, 394–408.

Bos, F. (1981). Optimization of spectral coverage in an eight-cell oscillator-amplifier dye laser pumped at 308 nm. *Appl. Opt.* **20**, 3553–3556.

Brivio, F., Mazzoleni, S. & Milani, M. (1993). Asymmetries and instabilities in a semiconductor laser with optical feedback. *Opt. Engin*. **32**, 705–712.

Brivio, F., Mazzoleni, S. & Milani, M. (1994). Asymmetrical response of semiconductor lasers in optical systems. *J. Theor. Math. Phys.* **99**, 364.

Chouffani, K., Harmon, F., Wells, D., Jones, J. & Lancaster, G. (2006). Laser-compton scattering as a tool for electron beam diagnostics. *Laser Part. Beams* **24**, 411–419.

Duarte, F.J. & Hillman, L.W. (1985). *Dye Laser Principles*. New York: Academic Press.

Fitzsimmons, W.A., Anderson, L.W., Riedhauser, C.E. & Vrtilek, Jan, M. (1976). Experimental and theoretical investigation of the nitrogen laser. *IEEE J Quan. Elec.* **12**, 624–633.

Godard, B. (1974). A simple high-power large-efficiency N2 ultraviolet laser. *IEEE J. Quan. Elec.* **10**, 147.

Jeunehomme, M. & Duncan, A.B.F. (1964). Lifetime measurements of some excited states of nitrogen, nitric oxide, and formaldehyde. *J. Chem. Phys*. **41**, 1692–1698.

Kahr, B. & Gurney, R.W. (2001). Dyeing crystals. *Chem. Rev*. **101**, 893–952.

Lin, Q.B. & Zhang, F.G. (1987). Coumarin 120 laser pulses close to the Fourier transform limit from a simplified resonant cavity. *Appl. Opt*. **26**, 2572–2574.

Milani, M., Costato, M., Morselli, S., Salsi, F., Ballerini, M., Baroni, G., Cozzi, S., Ferraro, L., Tallone, L., Bettega, D. & Calzolari, P. (1999). Coherent pulsed UV irradiation of yeast and HeLa cells: Short and long term effects. *Laser & Techn*. **8**, 8–14.

Milani, M., Ferraro, L., Baroni, G., Sozzani, P., Adobati, M. & Ravetta, S. (2000). High efficiency laser pumping system for magnetic resonance imaging. In *Biomedical Diagnostic,*

*Guidance, and Surgical assist Systems II (*TVo-Dinh T., W.S. Grundfest, W.S. and D.A. Benaron, D.A., Eds.) Vol. 3911, pp. 191–198. San Diego: SPIE.

Miley, G.H., Hora, H., Osman, F., Evans, P. & Toups, P. (2005). Single event laser fusion using ns-MJ laser pulses. *Laser Part. Beams* **23**, 453–460.

Rifani, M., Yin, Yi-Yan, Elliott, D.S., Jay, M.J., Jang Sei-Hum, Kelley, M.P., Bastin, L. & Kahr, B. (1995). Solid state dye lasers from stereospecific host-guest interactions. *J. Am. Chem. Soc*. **117**, 7572–7573.

Schwab, A.J. & Hollinger, F.W. (1976). Compact high-power N2 laser: Circuit theory and design. *IEEE J. Quan. Elec*. **12**, 183–188.

Strohwald, H. & Salzmann, H. (1976). Picosecond UV laser pulses from gas discharges in pure nitrogen at pressures up to 6 atm. *Appl. Phys. Lett*. **28**, 272–274.

Wolowski, J., Badziak, J., Czarnecka, A., Parys, P., Pisarek, M., Rosinski, M., Turan, R. & Yerci, S. (2007). Application of pulsed laser deposition and laser-induced ion implantation for formation of semiconductor nanocrystallites. *Laser Part. Beams* **25**, 65–69.